Geophys. J. Int. (1997) **129**, 691–701

Contribution of serpentinized ultramafics to marine magnetic anomalies at slow and intermediate spreading centres: insights from the shape of the anomalies

Jérôme Dyment,[1,2] Jafar Arkani-Hamed[1] and Abdolreza Ghods[1]

[1]*Earth and Planetary Sciences, McGill University, Montréal, Québec, Canada*

[2]*CNRS* UMR 6538, *Université de Bretagne Occidentale, Brest, France. E-mail: jerome@univ-brest.fr*

Accepted 1997 February 6. Received 1997 February 6; in original form 1996 March 14

SUMMARY

Detailed characteristics of marine magnetic anomalies 33r and 20r suggest that the magnetization of the deeper magnetic layers, including the lower crust and possibly the uppermost mantle, is horizontally displaced with respect to that of the upper crust. We examine the possibility that serpentinization of ultramafics in the lower crust and possibly the uppermost mantle delays the acquisition of magnetization and introduces a shift between the upper- and lower-crustal magnetization patterns. Thermal evolution models and the resulting magnetization patterns of the oceanic lithosphere are calculated for a wide range of physical parameters such as the Nusselt number and the depth of hydrothermal circulation in the crust, and the temperature range of serpentinization. The models with moderate hydrothermal cooling of the whole crust and serpentinization temperatures ranging between 200 and 300 °C successfully explain the anomalous skewness and the 'hook shape' of observed sea-level magnetic anomalies created at slow and intermediate spreading rates.

Key words: magnetic anomalies, magnetization, mid-ocean ridges, oceanic crust, oceanic lithosphere.

INTRODUCTION

Uncertainties remain on the source of seafloor-spreading magnetic anomalies. The standard magnetization model of the extrusive basaltic layer (e.g. Talwani, Windisch & Langseth 1971), with measured magnetization of oceanic basalts (e.g. Bleil & Petersen 1983), cannot explain the amplitude of the anomalies at sea level (e.g. Harrison 1987) and at satellite altitudes (Raymond & LaBrecque 1987; Toft & Arkani-Hamed 1992). It cannot produce the anomalous skewness of marine magnetic anomalies (Cande 1978; Roest, Arkani-Hamed & Verhoef 1992; Dyment, Cande & Arkani-Hamed 1994) and of satellite magnetic anomalies associated with the Cretaceous quiet zones in the North Atlantic Ocean (LaBrecque & Raymond 1985). Other magnetization models, including the decay of magnetization of the extrusive basaltic layer due to inferred geomagnetic intensity decrease (Cande 1978), crustal tectonic rotations (Verosub & Moores 1981), secondary magnetization of the extrusive layer (Raymond & LaBrecque 1987) and magnetization of the whole crust and possibly the uppermost mantle (Cande 1978; Arkani-Hamed 1988, 1989) may partly explain amplitude and anomalous skewness observations but cannot account for the observed relationship between anomalous skewness and spreading rates. Skewness analyses from various oceans show that the anomalous skewness of marine magnetic anomalies decreases with increasing spreading rate (Roest *et al.* 1992) and becomes negligible above a spreading rate of about 50 km Myr^{-1} (Dyment *et al.* 1994). These observations led Dyment & Arkani-Hamed (1995) to modify the thermoviscous remanent magnetization model of Arkani-Hamed (1989) in order to account for the spreading-rate dependence of the magnetic structure of the oceanic lithosphere. From the analysis of anomalies 33 reversed (33r) and 25 reversed (25r), they estimated that the contribution of the lower magnetic layers (i.e. the lower crust and possibly the uppermost mantle) to these marine magnetic anomalies progressively decreases from about 40 per cent at a spreading rate of 10 km Myr^{-1} to zero at spreading rates greater than 55 km Myr^{-1}. Such a variation of magnetization with spreading rate may result from the combined effects of parameters which most likely vary with spreading rate, such as magma fractionation, which affects the iron content of basalts (e.g. Niu & Batiza 1993), alteration of the extrusive basalts, which reduces their content of titanomagnetite (e.g. Bleil & Petersen 1983) and serpentinization of the deeper ultramafics, which produces magnetite in the deeper crust and possibly the uppermost mantle (e.g. Dunlop & Prevot 1982; Harrison 1987).

Pervasive tectonism associated with the style of accretion at slow and intermediate spreading centres (e.g. Macdonald 1982) results in a faulted and heterogeneous crust which is more easily penetrated by hydrothermal circulation and therefore more readily subject to alteration. Serpentinization, which is a low-temperature hydrothermal alteration that transforms olivine-rich rocks, such as lower-crustal gabbros or uppermost-mantle peridotites, to serpentinites, has been observed worldwide on oceanic rock samples dredged or drilled in non-fracture-zone settings at slow and intermediate spreading centres, whereas it is virtually absent in similar settings at fast spreading centres (Juteau, Cannat & Lagabrielle 1990; Cannat 1993). Widespread serpentinization has also been inferred from the chemical composition of seawater in the vicinity of active hydrothermal fields at the slow-spreading Mid-Atlantic Ridge (Bougault *et al.* 1993; Charlou & Donval 1993). Serpentinization may therefore be an important process at slow spreading centres (e.g. Francis 1981; Cannat 1993). Most of the chemical reactions proposed for serpentinization predict the production of secondary magnetite (see Toft, Arkani-Hamed & Haggerty 1990 for a review), a prediction largely confirmed by the observations (Coleman 1971; Bina & Henry 1990; Krammer 1990; Nazarova 1994). Unlike the low-temperature alteration of upper-crustal extrusive basalts, which reduces the magnetization by about an order of magnitude within approximately the first 20 Myr through decreasing their titanomagnetite content (e.g. Bleil & Petersen 1983), low-temperature serpentinization of gabbros and peridotites in the lower crust and the uppermost mantle can precipitate secondary magnetite and thus increase the magnetization. The magnetite produced by partial serpentinization of the lower crust and uppermost mantle is probably a major magnetic mineral there (Dunlop & Prévot 1982) and may contribute to marine magnetic anomalies (Harrison 1987; Hamano, Bina & Krammer 1990). Dyment & Arkani-Hamed (1995) modelled the acquisition of magnetization at blocking temperatures of 200–400 °C for the titanomagnetites of the extrusive basalts and 400–600 °C for the primary magnetite of the other layers. The acquisition of magnetization in the lower crust and possibly the uppermost mantle through serpentinization occurs at much lower temperatures (see discussion on serpentinization temperatures below). To account for the magnetization of the deeper layers acquired through low-temperature serpentinization, Dyment & Arkani-Hamed's (1995) model has to be modified.

Dyment & Arkani-Hamed's (1995) model explains the major characteristics of marine magnetic anomalies. However, it does not produce the detailed shape of observed anomalies for slow and intermediate spreading rates (10–40 km Myr^{-1} half-rate). Fig. 1 shows the deskewed magnetic anomaly 33r in the Central and South Atlantic Ocean and on the Southwest Indian Ridge, which displays symmetrical shoulders and, aside from minor details, a strongly asymmetrical central part with a maximum which is systematically shifted towards the younger side of the anomaly (Cande 1978). This 'hook shape' pattern (Cande 1993) is also observed on anomaly 20r in the North Atlantic (Roest *et al.* 1992, their Fig. 6) and on anomalies 20–22 in the Wharton Basin, Indian Ocean (Dyment *et al.* 1994, their Fig. 2). It is only discernible on relatively wide anomalies and is therefore more difficult to see at slow (< 25 km Myr^{-1}) than at intermediate (25–40 km Myr^{-1}) spreading rates. It does not exist on anomalies created at fast spreading rates (> 40 km Myr^{-1}). Cande (1993) suggested that a horizontal shift between a lower and an upper magnetic layer may explain both the 'hook shape' and the small anomalous skewness of anomalies M0–M4 (Cande & Kent 1985; Roest *et al.* 1992). The required shift for the 'hook shape' of anomaly 33r at a spreading rate of 35 km Myr^{-1} is about 25 km. This shift

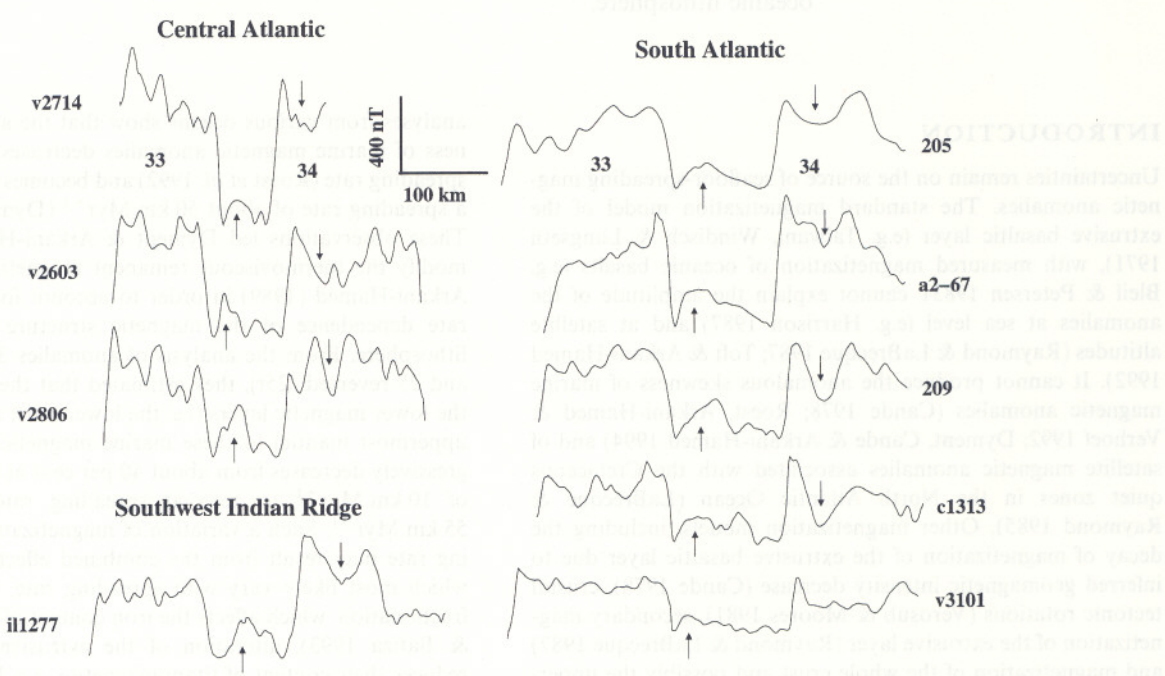

Figure 1. Marine magnetic anomalies 33–34 in the Central Atlantic, Southwest Indian Ridge and South Atlantic, phase-shifted to deskew anomaly 33r. Spreading rates range from 22 to 35 km Myr^{-1}. The 'hook shapes' of anomalies 33r and 34 are shown by arrows pointing upward and downward, respectively. Labels identify ships (v: R/V Vema; il: R/V Islas Orcadas; a2: R/V Atlantis II; c: R/V Conrad; numbers: aeromagnetic data) and legs.

cannot be produced by tectonic displacement of the lower crust with respect to the upper crust. This is because the displacement should occur after acquisition of magnetization, i.e. at temperatures lower than about 600 °C, and at these temperatures the oceanic crust is too strong to undergo substantial horizontal deformation to produce the required shift. The possible acquisition of secondary magnetization arising, for instance, from viscous processes does not produce any significant shift between the upper and lower magnetic layers (Arkani-Hamed 1989). Such an acquisition begins simultaneously with the acquisition of the primary magnetization, so the resulting magnetization pattern is similar to that of the thermal remanent magnetization. In order to produce a shift between the upper and lower magnetic layers and therefore give rise to the 'hook shape', it is necessary that the lower layers acquire part of their magnetization at a significantly later time. Such a later acquisition of magnetization in the lower crust and uppermost mantle can be the result of serpentinization. These layers require long periods of cooling from initially high temperatures to the temperatures of serpentinization, which may delay the acquisition of magnetization and thus introduce a shift between the magnetic pattern of the upper crust and that of the deeper layers. The importance of such a shift therefore depends on the thermal evolution of the oceanic lithosphere and the temperature range of serpentinization in the deeper layers, lower temperatures corresponding to larger shifts.

In this paper, we examine magnetization models of the oceanic lithosphere which take into account serpentinization of the lower crust and possibly the uppermost mantle. We do not consider other types of magnetization in these regions, such as thermoremanent and viscous magnetizations, although they may be important, in order to single out the effects of serpentinization. It is shown that low-temperature serpentinization can give rise to the 'hook shape' of anomalies 33r and 20r and produce anomalous skewness for anomalies 33r and 25r in good agreement with the observations.

MODELLING

A reliable modelling of the magnetization pattern of the oceanic lithosphere requires good knowledge about the thermal evolution and magnetic properties of the lithospheric layers, such as the dominant magnetic minerals and their magnetic blocking temperatures and saturation magnetizations. By saturation magnetization we mean the magnetization that would be acquired after an infinite time under a constant-polarity geomagnetic field. We conducted a systematic investigation of the physical parameters that could affect the resulting magnetization pattern in order to identify the dominant parameters. The thermal evolution of the oceanic lithosphere is calculated by solving the time-dependent 1-D heat-conduction equation taking into account a temperature-dependent thermal conductivity and the hydrothermal circulation in the crust, following the procedure adopted by Arkani-Hamed (1988). The effect of hydrothermal cooling is accounted for by multiplying the thermal conductivity of the hydrothermal layer by the Nusselt number of the hydrothermal convection. It is assumed that the Nusselt number decreases exponentially with time as the convection decays due to filling of the cracks by hydrothermal deposits, and reduces to 1 as the circulation completely ceases after 50 Myr (Stein & Stein 1992). We examine several models

Table 1. Parameters used to model the thermal evolution of the oceanic lithosphere.

Thickness of oceanic lithosphere	$95 \times 10^{+3}$ m
Thickness of oceanic crust	$6 \times 10^{+3}$ m
Density of lithosphere	$2.9 \times 10^{+3}$ kg m^{-3}
Specific heat of lithosphere	1200 J kg^{-1} K^{-1}
Temperature at the base of the lithosphere	1450 °C
Temperature at the top of the lithosphere	0 °C
Heat flow in old oceans (steady state)	50×10^{-3} W m^{-2}
Thickness of radiogenic heat-source layer	$6 \times 10^{+3}$ m
Depth of hydrothermal layer	$0–6 \times 10^{+3}$ m
Nusselt number	1–8
Duration of the hydrothermal effect	$50 \times 10^{+6}$ yr

with hydrothermal layer thicknesses of $D = 0$ (no hydrothermal layer), 2, 4 and 6 km, and initial Nusselt numbers of $v = 1$ (no hydrothermal layer), 1.5, 2.5, 5 and 9. Other thermal parameters (Table 1) are adopted from Arkani-Hamed (1988) and Stein & Stein (1992).

We assume a 12 km thick magnetic layer that includes the extrusive upper crust, the intrusive middle crust, the lower crust and the uppermost mantle, with thicknesses fixed at 0.5, 1.5, 4.0 and 6.0 km, respectively. Titanomagnetite and magnetite are considered as the major magnetic minerals of the extrusive upper crust and the deeper layers, respectively (Dunlop & Prévot 1982). A magnetic blocking temperature range of 160–420 °C is assumed for the titanomagnetites and 520–580 °C for the magnetite. The magnetization of the upper crust is essentially primary thermoremanent magnetization (TRM), because it cools very rapidly, and is modelled following Arkani-Hamed (1988). In order to single out the effect of serpentinization, we adopt the hypothesis that all of the magnetite in the lower crust and uppermost mantle is produced by serpentinization, although some primary magnetite may exist (e.g. Pariso & Johnson 1993). No viscous magnetization was considered because (1) due to its strong temperature dependence, the viscous magnetization of magnetite is relatively small for temperatures lower than 400 °C (Pullaiah *et al.* 1975), and (2) the viscous magnetization acquired since the last core field polarity reversal by the lower crust and uppermost mantle of the oceanic lithosphere older than about 30 Myr is essentially uniform horizontally and has little effect on the short-wavelength marine magnetic anomalies (Arkani-Hamed 1989). Like other hydrothermal alterations, serpentinization is controlled by the existing faults, cracks and microcracks. With a moderate number of cracks within a kilometre on the horizontal scale, discrete serpentinized zones resemble a zone of uniform serpentinization as far as their magnetic signature at sea level is concerned: the magnetic anomalies of individual serpentinized zones significantly overlap as the anomalies are continued upward from the depth of the lower crust to sea level, by more than 8 km in our models.

The temperature range of serpentinization controls the time lag between the acquisition of magnetization within the upper and lower magnetic layers. It is, however, difficult to constrain this essential parameter because (1) although numerous processes are proposed (see Toft *et al.* 1990 for a review), the appropriate chemical reaction to describe serpentinization of the oceanic lower crust and uppermost mantle is still to be determined, (2) there are insufficient thermodynamic data to constrain the pressure–temperature dependence of these

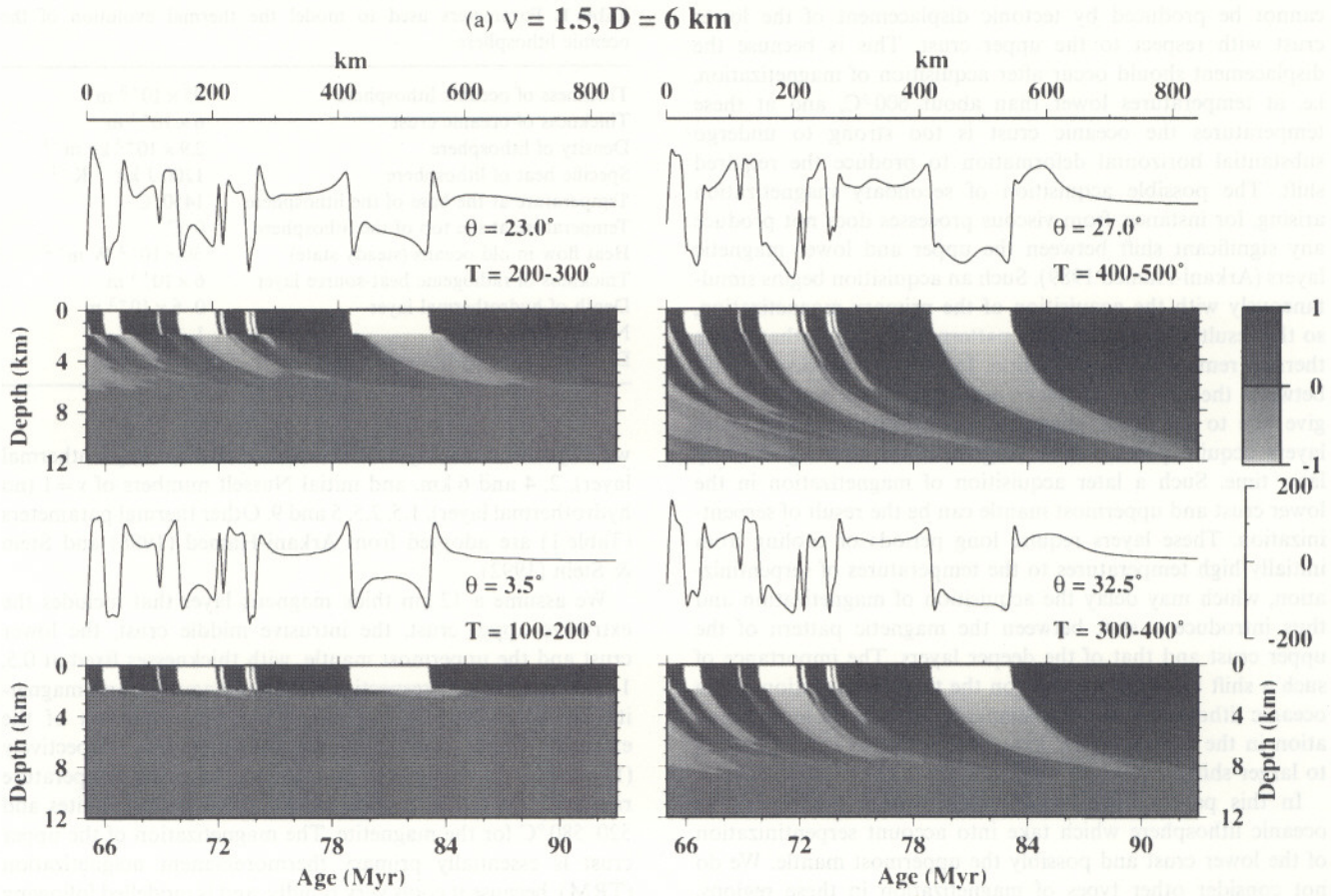

Figure 2. Normalized magnetization patterns for varying lower bound (a) and width (b) of the serpentinization temperature range, depth of the hydrothermal layer (c) and initial Nusselt number of the hydrothermal convection (d), other parameters being kept constant. The magnetization patterns are normalized to a maximum value of 1 A m^{-1} in order to enhance details of magnetization of the lower layers for visual clarity. Normalized magnetizations have to be multiplied by the saturation magnetization of the corresponding layer before computation of synthetic magnetic anomalies. Also shown are synthetic magnetic anomalies at sea level produced by the magnetization distribution model assuming a 6 km water depth, a 35 km Myr^{-1} spreading rate and saturation magnetizations of 6, 0.5, 2 and 0 A m^{-1} for the extrusive upper crust, the intrusive upper crust, the lower crust and the uppermost mantle, respectively. θ is the phase-shift required to deskew anomaly 33r. T is the serpentinization temperature range, D is the depth of the hydrothermal layer and ν is the initial Nusselt number of the hydrothermal convection.

reactions, and (3) many factors, such as the initial composition of the rocks, the water and CO_2 content and the lithostatic pressure, may affect this parameter (Wicks & O'Hanley 1988). For the most common oceanic lizardite–chrysotile assemblage, oxygen isotope measurements suggest a temperature range of 130–185 °C (Wenner & Taylor 1971) or 30–200 °C (Bonatti, Lawrence & Morandi 1984). However, these may be too low by as much as 100 °C (Moody 1976) because of the simplifying assumptions made to build the serpentine–magnetite geothermometer (Bottinga & Javoy 1973). Temperatures of 200–350 °C were recently reported (Agrinier *et al.* 1995). Various pressure–temperature experiments suggest that these minerals may be stable at temperatures lower than 425 °C (Caruso & Chernosky 1979) or 325 °C (Elthon 1981; Krammer 1990). Bideau *et al.* (1991) concluded that serpentinization may begin between 200 °C and 400 °C and continue below 200 °C. Serpentinization requires the presence of water. The oceanic crust created at slow and intermediate spreading rates is strongly tectonized, and sea water may reach the deeper parts along normal faults. Evidence for hydrothermal circulation is observed at the ridge axis at temperatures much higher than that required for serpentinization (e.g. Gillis, Thompson & Kelley 1993; Nehlig 1993). Pervasive serpentinization may only happen if the hydrothermal fluids diffuse through the lower-crustal and uppermost-mantle ultramafics. The water pressure and transport coefficients are, however, strongly temperature-dependent, and so is the rate of pervasive serpentinization. Macdonald & Fyfe (1985) have shown that serpentinization is a fairly rapid process for temperatures higher than 100 °C; below 100 °C, the rate of serpentinization is too low to ensure pervasive serpentinization. For these reasons, we consider the temperature (and not water influx) as the controlling parameter of serpentinization.

We examine serpentinization temperatures between 100 and 500 °C, which include most of the values in the literature (Toft *et al.* 1990). Serpentinization is assumed to be significant within a given temperature range and independent of pressure, and it increases linearly as temperature decreases within that range. Five different ranges of 50, 100, 200, 300 and 400 °C are examined, with a total of 14 serpentinization models: four models with a temperature range of 50 °C (100–150 °C, 200–250 °C, ...), four models with a temperature range of 100 °C (100–200 °C, 200–300 °C, ...), three models with a temperature range of 200 °C (100–300 °C, 200–400 °C, ...), two models with

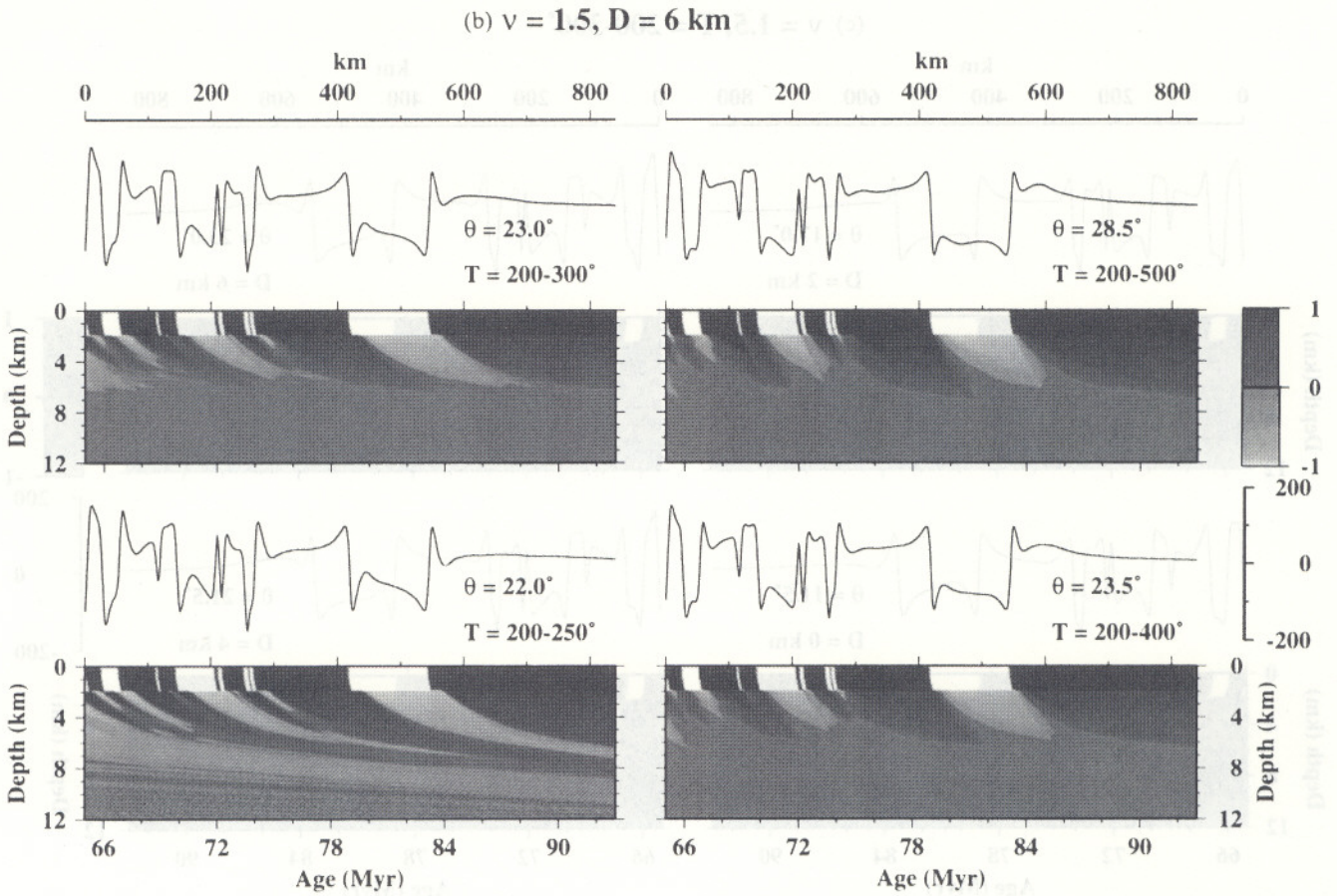

Figure 2. (*Continued.*)

a temperature range of 300 °C (100–400 °C, 200–500 °C), and one model with a temperature range of 400 °C (100–500 °C). We monitored the temperature of a given volume element of the oceanic lithosphere. When the temperature falls inside the serpentinization temperature range, magnetization is acquired in proportion to the degree of serpentinization and in the direction of the prevailing core field, similar to the process described by Arkani-Hamed (1988) for TRM acquisition.

Magnetic anomalies corresponding to the resulting magnetization models of the oceanic lithosphere are calculated at sea level assuming a constant bathymetry of 6 km and slow (10 km Myr^{-1}) to intermediate (35 km Myr^{-1}) spreading rates. The magnetization vector is assumed to be vertical and the anomalies are determined at the North geomagnetic pole to avoid unnecessary mathematical manipulations arising from inclined magnetization and geomagnetic field vectors. Saturation magnetizations of 6.0 and 0.5 A m^{-1} are assigned for the extrusive upper crust and intrusive middle crust, respectively, in all of the models. We examine different saturation magnetizations for the lower crust and uppermost mantle, varying between 0 and 2 A m^{-1}, like most of the values proposed in the literature (see Toft & Arkani-Hamed 1992 for a review). The effect of each physical parameter is examined based on the constraints that (1) the anomalous skewness of the synthetic marine magnetic anomalies 33r and 25r agrees with that observed at a spreading rate of 35 km Myr^{-1}, i.e. $27° \pm 4°$ and $15° \pm 7°$, respectively (Roest *et al.* 1992; Dyment *et al.* 1994), and (2) the 'hook shape' of anomalies 33r and 20r is produced.

In addition, we try to ensure a relatively small anomalous skewness for anomalies M0–M4, as has been suggested from studies in the Atlantic Ocean (Cande 1978; Roest *et al.* 1992). We do not put too much emphasis on this observation, however, as anomalies M0–M4 lack an essential quality to provide unambiguous anomalous skewness measurements. Unlike anomalies 33r, 25r and 20r, which are associated with simple and roughly symmetrical polarity sequences, anomalies M0–M4 correspond to the complex combination of two relatively long polarity intervals with several shorter intervals. The shape of the anomalies is significantly altered by slight modifications in the size of these shorter intervals, which may arise from small ridge jumps, for instance (compare profiles V2412, V2206, and C1314 in Fig. 8 of Cande 1978). A systematic study is clearly required to investigate the consequences of this 'sequence effect' (Dyment *et al.* 1994) on the value and dispersion of the anomalous skewness of anomalies M0–M4. Simple geometrical considerations suggest that the slower the spreading rate the more effective the 'sequence effect' is on the shape and anomalous skewness of the anomalies (Dyment *et al.* 1994). For this reason, we only consider the anomalous skewness of anomalies M0–M4 predicted by the models for a spreading rate of 35 km Myr^{-1}, and do not take slower rates into consideration. Another reason to treat synthetic anomalies M0–M4 with caution is the poorly constrained

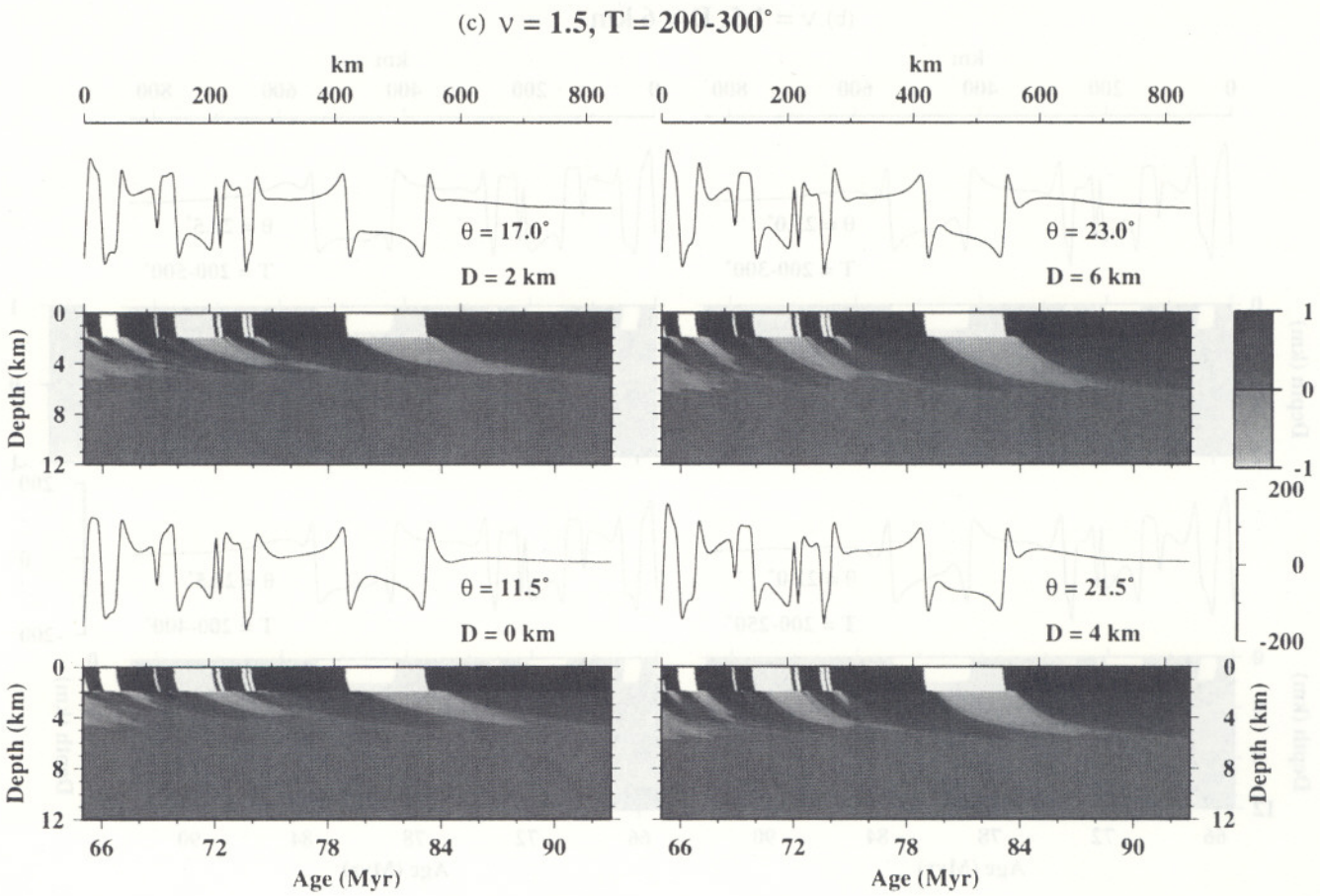

Figure 2. (*Continued.*)

(both in absolute age and relative duration of the polarity intervals) geomagnetic polarity time scale for the Mesozoic anomalies.

RESULTS

Figs 2(a)–(d) show the magnetization patterns produced for various temperatures of serpentinization, temperature ranges of serpentinization, depths of the hydrothermal layer, and Nusselt numbers, respectively. As expected, low temperatures of serpentinization produce larger shifts between the upper- and lower-crustal magnetization patterns, because the lower-crustal rocks take longer to cool and become serpentinized and thus acquire magnetization (Figs 2a and b). Assuming no hydrothermal cooling, $\nu = 1$, a serpentinization temperature range of 200–300 °C ensures a sufficient shift to produce the 'hook shape' of anomalies 33r and 20r and a small anomalous skewness for anomalies M0–M4 at a spreading rate of 35 km Myr^{-1}. However, the anomalous skewness of anomalies 33r and 25r produced by this model using a reasonable saturation magnetization of the lower crust (about 2 A m^{-1}) is less than the observed one. This is because the lower-crustal rocks gradually acquire magnetization during several polarity intervals, resulting in diffuse, weak and shallow (<4 km) magnetization patterns (Fig. 2c, $D = 0$ km, Fig. 2d, $\nu = 1$). Faster acquisition of magnetization in the lower crust can be achieved through rapid cooling. We therefore investigate the effect of hydrothermal cooling using different thicknesses of the hydrothermal layer and different initial Nusselt numbers (Figs 2c and d). Models with thin hydrothermal layers (the upper crust only, $D < 2$ km) yield almost the same results as those with no hydrothermal cooling, with anomalous skewness of anomalies 33r and 25r less than the observed one. The resulting anomalous skewness increases as the hydrothermal layer includes thicker parts of the lower crust ($D > 2$ km, Fig. 2c). Models with thicker hydrothermal layers (the whole oceanic crust, $D =$ 6 km, Fig. 2c) successfully produce the 'hook shape' of anomalies 33r and 20r, the anomalous skewness of anomalies 33r and 25r, and a small anomalous skewness for anomalies M0–M4 at a spreading rate of 35 km Myr^{-1} for low initial Nusselt numbers ($\nu = 1.5$, Fig. 2d). As the initial Nusselt number increases the models at first do not generate any 'hook shape' ($\nu \geq 2$) and then do not produce a significant anomalous skewness for anomalies 33r and 25r ($\nu \geq 4$). This is because at higher Nusselt numbers the shift between the upper- and lower-crustal magnetization patterns is reduced and the magnetic polarity transition boundaries become progressively vertical and sharp. Therefore, models with moderate hydrothermal cooling ($\nu = 1.5$–2.0) in most of the oceanic crust ($D = 4$–6 km) may account for the anomalous skewness of anomalies 33r and 25r and for the 'hook shape' of anomalies 33r and 20r. It also predicts a small anomalous skewness for anomalies M0–M4 at a spreading rate of 35 km Myr^{-1}. We consider a thermal evolution model with moderate hydrothermal cooling of the whole crust ($\nu = 1.5$, $D = 6$ km) a suitable model, and proceed to investigate the effects of different temperature ranges of serpentinization.

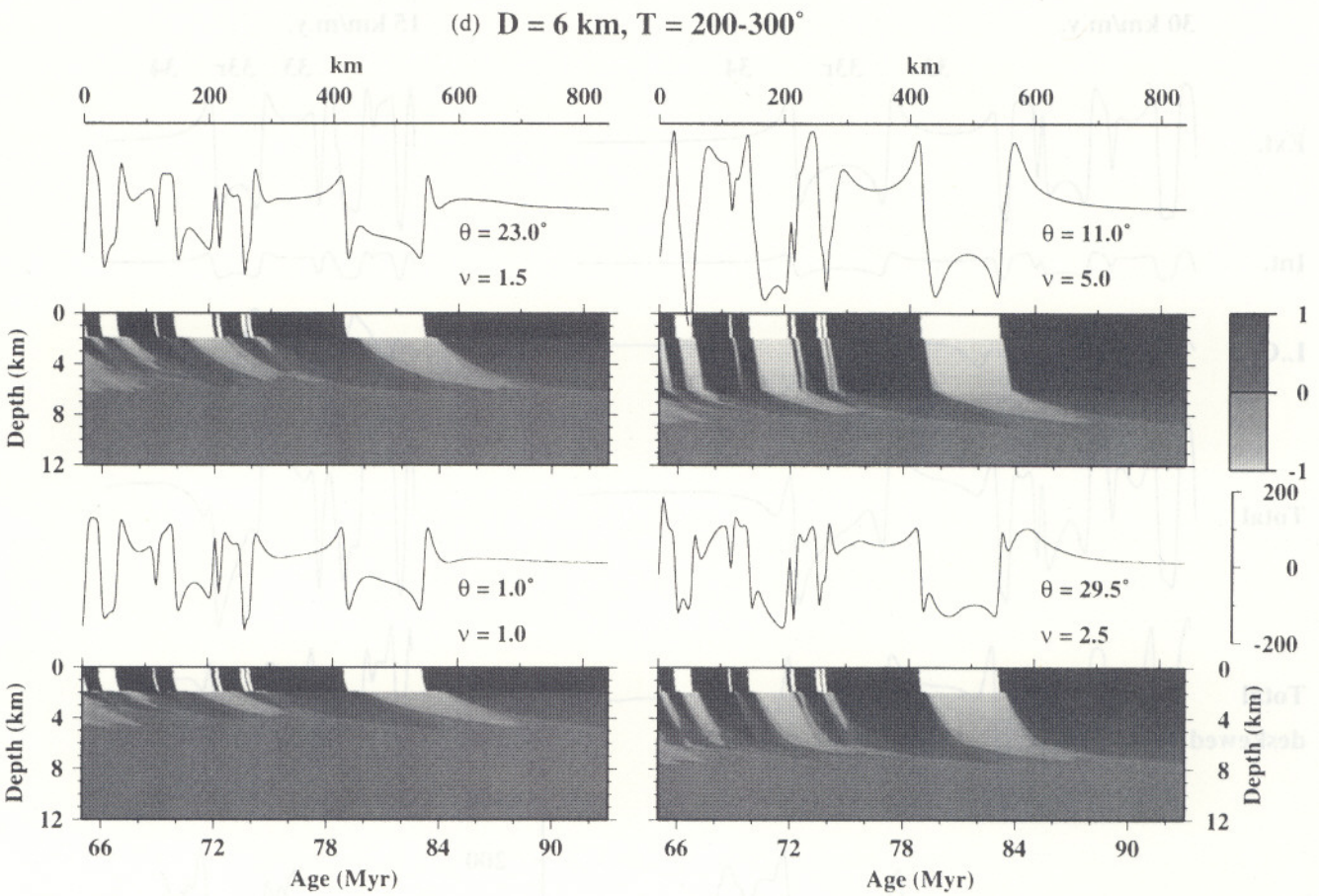

Figure 2. (*Continued.*)

Models with serpentinization temperatures less than 200 °C are unable to produce the anomalous skewness of anomalies 33r and 25r and the 'hook shape' of anomalies 33r and 20r because such low serpentinization temperatures drastically reduce the contribution of the lower crust to the synthetic magnetic anomalies (Fig. 2a, $T_0 = 100$ °C). Those with serpentinization temperatures greater than 400 °C fail to produce the 'hook shape' of anomalies 33r and 20r because such high-temperature serpentinization produces a magnetization pattern similar to that of TRM, without a significant shift between the upper and lower magnetic layers (Fig. 2a, $T_0 = 400$ °C). Serpentinization temperatures in the interval 200–400 °C successfully produce the anomalous skewness and the 'hook shape' of the anomalies (Fig. 2a) within the tolerance of the available data (Fig. 1). The anomalous skewness of the synthetic anomalies 33r and 25r can be adjusted by changing the saturation magnetization of the lower crust with respect to that of the extrusive upper crust. On the other hand, the small anomalous skewness of anomalies M0–M4 at a spreading rate of 35 km Myr^{-1} is more sensitive to the shift between the upper- and lower-crustal magnetization patterns. Models with serpentinization temperature ranges of 200–250 °C and 200–300 °C create appropriate magnetization shifts and produce small anomalous skewnesses for these anomalies.

The magnetization of the uppermost mantle has little effect on the amplitude, anomalous skewness and 'hook shape' of the sea-level magnetic anomalies, a conclusion also reached for thermoremanent and thermoviscous remanent magnetization models of the oceanic lithosphere (Arkani-Hamed 1989). Serpentinization, and therefore the acquisition of magnetization, in the uppermost mantle is a slow process during which the geomagnetic field polarity may change several times. This results in a diffused magnetization pattern which has a negligible contribution to the short-wavelength marine magnetic anomalies, regardless of the intensity of the saturation magnetization. The uppermost mantle, however, may significantly contribute to the intermediate-wavelength (between 400 and 2500 km) magnetic anomalies observed at satellite altitudes.

Fig. 3 shows the magnetization patterns of the oceanic lithosphere corresponding to anomalies 29–34 determined using a 6 km thick hydrothermal layer, an initial Nusselt number of 1.5 and a serpentinization temperature range of 200–250 °C. Computations are carried out for spreading rates of 30 and 15 km Myr^{-1}. The observed magnetic anomaly profiles are also shown for comparison. The magnetization patterns of the upper and lower crust are shifted by about 0.7 Myr (i.e. 20 and 10 km at spreading rates of 30 and 15 km Myr^{-1}) at a depth of 2 km. Included in the figure are the magnetic anomaly contributions of the extrusive upper crust, the intrusive middle crust, the lower crust and the total magnetic anomaly calculated using saturation magnetizations of 6, 0.5 and 2 A m^{-1} for these layers, respectively. The 'hook shape' predicted by the model for deskewed anomalies 33r (Fig. 3, $\theta = 25°$ and 36° for spreading rates of 30 and

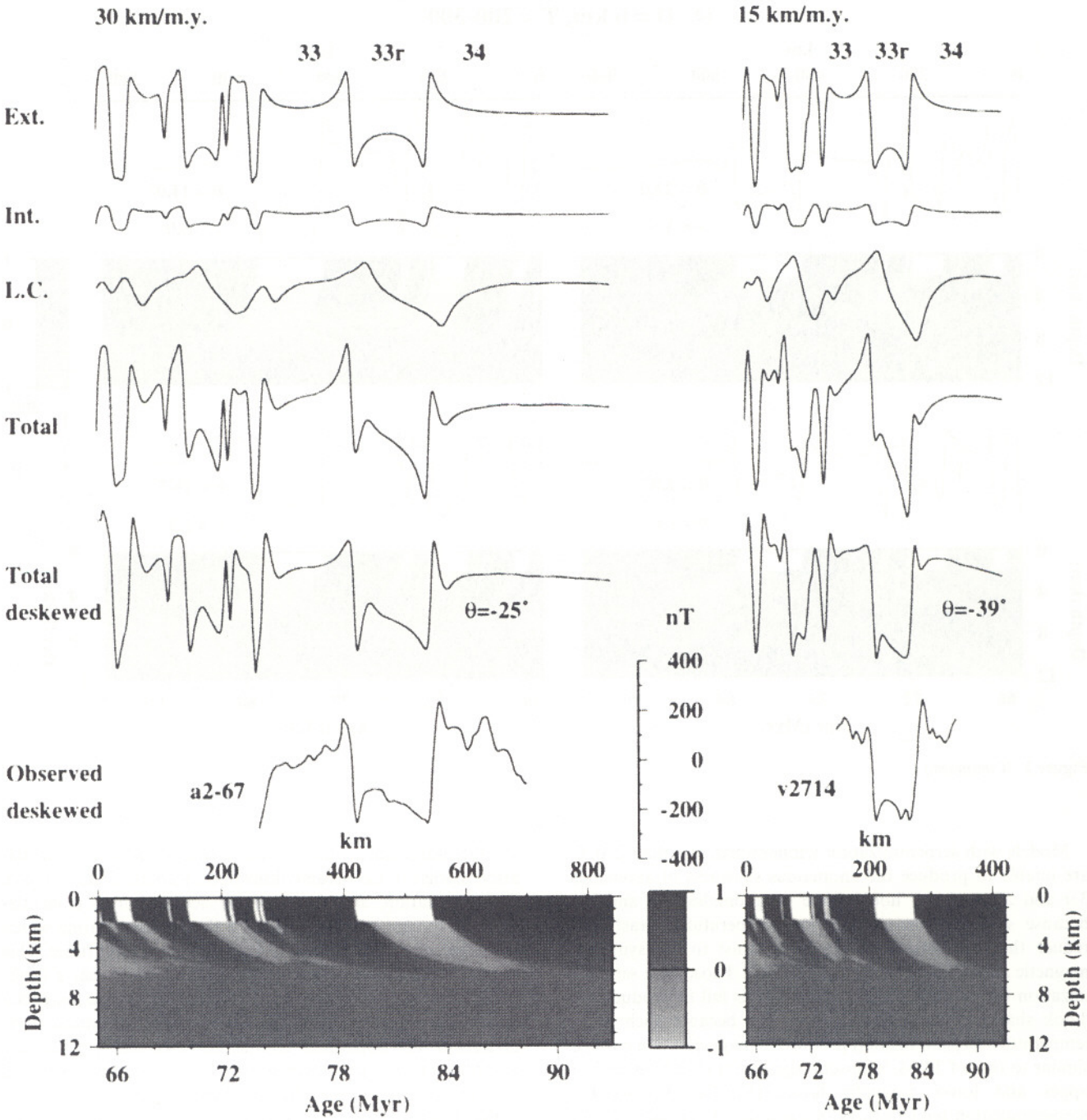

Figure 3. Normalized magnetization pattern (bottom) and synthetic magnetic anomalies at sea level (top) for anomalies 29–34 produced by the model for a serpentinization temperature range of 200–300 °C, a depth of the hydrothermal layer of 6 km and an initial Nusselt number of the hydrothermal convection of 1.5. The magnetization patterns are normalized to a maximum value of 1 A m^{-1} in order to enhance details of magnetization of the lower layers for visual clarity. Normalized magnetizations have to be multiplied by the saturation magnetization of the corresponding layer before computation of synthetic magnetic anomalies. Synthetic anomaly curves are, from top to bottom, the contribution of the extrusive upper crust, the intrusive upper crust, the lower crust, the total magnetic anomaly and the total anomaly phase-shifted by θ to deskew anomaly 33r. Examples of observed magnetic anomalies 33–34 (Roest *et al.* 1992) are shown for comparison. Spreading rates for modelled and observed anomalies 33–34 are 30 km Myr^{-1} (left) and 15 km Myr^{-1} (right).

15 km Myr^{-1}, respectively) is in good agreement with the observed data (Fig. 1, arrows). Similarly our model results in the 'hook shape' for anomaly 20r.

The synthetic anomalies M0–M6 computed for a spreading rate of 35 km Myr^{-1} (Fig. 4, top) show small anomalous skewnesses for anomalies M0 and M1 and a slightly larger one for anomaly M4. However, this result, which seems to agree with the observations of Cande & Kent (1985) and Roest *et al.* (1992), is probably coincidental. At this spreading rate, the effect of the narrow structures associated with the short

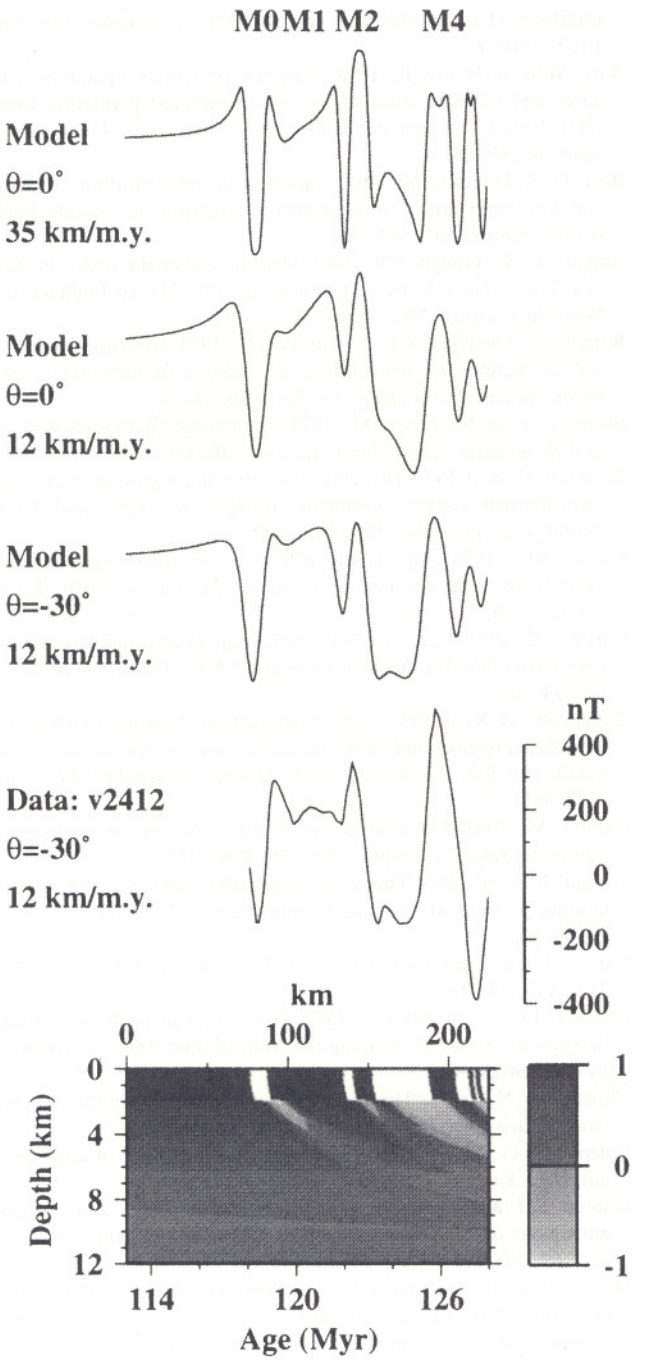

Figure 4. Normalized magnetization pattern (bottom) and synthetic magnetic anomalies at sea level (top) for anomalies M0–M6 produced by the model for a serpentinization temperature range of 200–300 °C, a depth of the hydrothermal layer of 6 km and an initial Nusselt number of the hydrothermal convection of 1.5. The magnetization patterns are normalized to a maximum value of 1 A m^{-1} in order to enhance details of magnetization of the lower layers for visual clarity. Synthetic anomaly curves are, from top to bottom, computed for spreading rates of 35 and 12 km Myr^{-1}. An example of observed magnetic anomalies M0–M4 at a spreading rate of 12 km Myr^{-1} (Cande & Kent 1985) is shown for comparison.

polarity intervals balance the effect of the lower-crustal dipping 'tails' corresponding to the larger polarity intervals. At a slow spreading rate, a significant anomalous skewness is obtained by the model, in agreement with some anomaly data (Fig. 4).

DISCUSSION AND CONCLUSIONS

Our modelling exercise suggests that serpentinization of the oceanic lower crust can successfully explain the 'hook shape' of anomalies 33r and 20r and the anomalous skewness of anomalies 33r and 25r. It may also account for the small anomalous skewness of anomalies M0–M4 at a spreading rate of 35 km Myr^{-1}. In our models the 'hook shape' of anomalies 33r and 20r is a direct consequence of the time lag between the acquisition of TRM in the upper crust and the low-temperature serpentinization, and thus the acquisition of magnetization, in the lower crust. Extensive modelling suggests that moderate hydrothermal circulation inside the entire crust and a serpentinization temperature range of about 200–300 °C produce favourable magnetization patterns.

An underlying assumption in our models is that serpentinization is a common process in the lower crust. However, it does not have to be very pervasive, as the linear relationship between the density (and therefore the amount of serpentine) and the logarithm of the magnetic susceptibilities of serpentinized peridotites (Coleman 1971; Toft *et al.* 1990) implies that moderate serpentinization may substantially increase the magnetization. The ultramafics recovered in non-fracture-zone settings at slow and intermediate spreading centres are indeed serpentinized (see Cannat 1993 for a review). The degree of serpentinization ranges from 20 to 80 per cent for samples of peridotites dredged from the seafloor (Bonatti & Hamlyn 1981). For most of the samples, however, there is no definitive distinction that they are serpentinized in deeper parts of the crust or closer to the seafloor. Serpentinites collected on the seafloor tend to equilibrate with the surrounding seawater and lose the memory of their initial alteration in deeper regions. Oxygen isotope studies of rocks from the Samail ophiolites (presumably created at a fast spreading rate) have shown that 'pervasive hydrothermal exchange with sea water occurred throughout the upper 75 per cent of this 8 km thick oceanic crustal section', and that seawater locally penetrated the tectonized peridotites (Gregory & Taylor 1981). Petrological analysis of altered gabbros and peridotites dredged from the equatorial Atlantic fracture zones suggests that the alteration 'took place in the deeper parts of the oceanic crust' (Honnorez & Kirst 1975). This direct (although local) evidence of *in situ* serpentinization is reinforced by more regional (although indirect) evidence. The numerous ultramafic outcrops observed on the extensively surveyed Mid-Atlantic Ridge south of the Kane Fracture Zone (22–24°N) are systematically associated with large zones (>10 km) of ridge-segment discontinuities and may reflect low magma supply and the quasi-absence of a magmatic crust at the ends of ridge segments (Cannat *et al.* 1995; Gente *et al.* 1995). Seismic and gravity studies support a 4–5 km thick crust of normal seismic velocity and density in these areas (e.g. Morris & Detrick 1991), suggesting that partial serpentinization has lowered the density and seismic velocity of the ultramafics over several kilometres depth. The seismic velocities of gabbros and peridotites that have been serpentinized up to 40 per cent are indistinguishable (Christensen 1972; Horen, Zamora & Dubuisson 1996).

The 'hook shape' of marine magnetic anomalies is only observed at slow and intermediate spreading rates, up to about 40 km Myr^{-1}. Similar anomalies created at fast spreading rates do not exhibit this characteristic, so the inferred shift between the upper and lower magnetic layers is only required at slow

and intermediate spreading rates. The anomalous skewness of marine magnetic anomalies decreases with increasing spreading rate and becomes negligible for spreading rates faster than 50 km Myr^{-1} (Dyment *et al.* 1994). Again, the lower-crustal magnetization 'tails' dipping away from the ridge are only required at slow and intermediate spreading rates. Therefore, pervasive serpentinization (as we have modelled it) may only be an important process at these spreading rates, in agreement with the petrological observations. With increasing spreading rates, the decreasing anomalous skewness requires a progressively weaker magnetization of the lower magnetic layer with respect to that of the upper magnetic layer. The absence of anomalous skewness and 'hook shape' at fast spreading rates (> 50 km Myr^{-1}) suggests a distribution of magnetization roughly similar to the standard rectangular prisms of constant magnetization with an alternating polarity in the extrusive upper crust (e.g. Talwani *et al.* 1971).

In this paper we have specifically modelled the effect of serpentinization and shown that it may explain both the anomalous skewness and the 'hook shape' of marine magnetic anomalies observed at slow and intermediate spreading rates. In order to single out the effects of serpentinization, we have not considered other types of magnetization such as thermoremanent and viscous magnetizations in the lower crust and uppermost mantle, although they may be important. Our results reinforce the conclusions of Dyment & Arkani-Hamed (1995) that (1) the magnetization of the extrusive upper crust is dominant at all spreading rates and (2) at slow and intermediate spreading rates, the magnetization of the serpentinized ultramafic rocks in the lower crust is a likely source of the anomalous skewness of the marine magnetic anomalies.

ACKNOWLEDGMENTS

This research was supported by the Natural Sciences and Engineering Research Council (NSERC) of Canada through Operating Grant OGP0041245 to JAH and by the Centre National de la Recherche Scientifique–Institut National des Sciences de l'Univers (CNRS–INSU) through a grant from 'Programme Dorsales — Appel d'Offre Modélisation Physique et Chimique du Comportement du Manteau sous les Dorsales Océaniques' to JD. At the initial stage of this project, JD was supported by a NSERC International Fellowship. AG was supported by a scholarship from the Ministry of Higher Education of Iran. Many discussions with Steve Cande about the 'hook shape' of marine magnetic anomalies are gratefully acknowledged. Thanks are also due to Daniel Bideau and an anonymous reviewer for their comments.

REFERENCES

Agrinier, P, Hekinian, R., Bideau, D. & Javoy, M., 1995. O and H stable isotope compositions of oceanic crust and upper mantle rocks exposed in the Hess Deep near the Galapagos Triple Junction, *Earth planet. Sci. Lett.*, **136,** 183–196.

Arkani-Hamed, J., 1988. Remanent magnetization of the oceanic upper mantle, *Geophys. Res. Lett.*, **15,** 48–51.

Arkani-Hamed, J., 1989. Thermoviscous remanent magnetization of oceanic lithosphere inferred from its thermal evolution, *J. geophys. Res.*, **94,** 17 421–17 436.

Bideau, D., Hebert, R., Hekinian, R. & Cannat, M., 1991. Metamorphism of deep-seated rocks from the Garrett ultrafast transform (East Pacific Rise near 13°25′S), *J. geophys. Res.*, **96,** 10 079–10 099.

Bina, M.M. & Henry, B., 1990. Magnetic properties, opaque mineralogy and magnetic anisotropies of serpentinized peridotites from ODP Hole 670 A near the Mid-Atlantic Ridge, *Phys. Earth planet. Inter.*, **65,** 88–103.

Bleil, U. & Petersen, N., 1983. Variation in magnetization intensity and low temperature titanomagnetite oxidation of oceanic floor basalts, *Nature,* **301,** 384–388.

Bonatti, E. & Hamlyn, P.R., 1981. Oceanic ultramafic rocks, in *The Sea,* Vol. 7, *The Oceanic Lithosphere,* pp. 489–524, ed Emiliani, C., Wiley-Interscience, New York, NY.

Bonatti, E., Lawrence, J.R. & Morandi, N., 1984. Serpentinization of oceanic peridotites: temperature dependence of mineralogy and boron content, *Earth planet. Sci. Lett.*, **70,** 88–94.

Bottinga, Y. & M. Javoy, M., 1973. Comments on oxygen isotope geothermometry, *Earth planet. Sci. Lett.*, **20,** 250–265.

Bougault, H. *et al.* 1993. Fast and slow spreading ridges: structure and hydrothermal activity, ultramafic topographic highs, and CH4 output, *J. geophys. Res.*, **98,** 9643–9651.

Cande, S.C., 1978. Anomalous behaviour of paleomagnetic field inferred from the skewness of anomalies 33 and 34, *Earth planet. Sci. Lett.*, **40,** 275–286.

Cande, S.C., 1993. Can a mid-tow survey tell us anything new about the source of marine magnetic anomalies? *EOS, Trans. Am. geophys. Un.*, **74,** 217.

Cande, S.C. & Kent, D.V., 1985. Comment on 'Tectonic rotations in extensional regimes and their paleomagnetic consequences for ocean basalts' by K.L. Verosub & E.M. Moores, *J. geophys. Res.*, **90,** 4647–4651.

Cannat, M., 1993. Emplacement of mantle rocks in the seafloor at mid-ocean ridges, *J. geophys. Res.*, **98,** 4163–4172.

Cannat, M. *et al.* 1995. Thin crust, ultramafic exposures, and rugged faulting patterns at the Mid-Atlantic Ridge (22°–24°N), *Geology,* **23,** 49–52.

Caruso, L.J. & Chernosky, J.V., 1979. The stability of lizardite, *Can. Min.*, **17,** 757–769.

Charlou, J.L. & Donval, J.P., 1993. Hydrothermal methane venting between 12°N and 26°N along the Mid-Atlantic Ridge, *J. geophys. Res.*, **98,** 9625–9642.

Christensen, N.I., 1972. The abundance of serpentinites in the oceanic crust, *J. Geol.*, **80,** 709–719.

Coleman, R.G., 1971. Petrologic and geophysical nature of serpentinites, *Geol. Soc. Am. Bull.*, **82,** 897–918.

Dunlop, D.J. & Prévot, M., 1982. Magnetic properties and opaque mineralogy of drilled submarine intrusive rocks, *Geophys. J. R. astr. Soc.*, **69,** 763–802.

Dyment, J. & Arkani-Hamed, J., 1995. Spreading-rate-dependent magnetization of the oceanic lithosphere inferred from the anomalous skewness of marine magnetic anomalies, *Geophys. J. Int.*, **121,** 789–804.

Dyment, J., Cande, S.C. & Arkani-Hamed, J., 1994. Skewness of marine magnetic anomalies created between 85 and 40 Ma in the Indian Ocean, *J. geophys. Res.*, **99,** 24 121–24 134.

Elthon, D., 1981. Metamorphism in oceanic spreading centers, in *The Sea,* Vol. 7, *The Oceanic Lithosphere,* pp. 285–303, ed Emiliani, C., Wiley-Interscience, New York, NY.

Francis, T.J.G., 1981. Serpentinization faults and their role in the tectonics of slow spreading ridges, *J. geophys. Res.*, **86,** 11 616–11 622.

Gente, P. *et al.* 1995. Characteristics and evolution of the segmentation of the Mid-Atlantic Ridge between 20°N and 24°N during the last 10 million years, *Earth planet. Sci. Lett.*, **129,** 55–71.

Gillis, K.M., Thompson, G. & Kelley, D.S., 1993. A view of the lower crustal component of hydrothermal systems at the Mid-Atlantic Ridge, *J. geophys. Res.*, **98,** 19 597–19 619.

Gregory, R.T. & Taylor, H.P., 1981. An oxygen isotope profile in a section of Cretaceous ocean crust, Samail ophiolite, Oman: evidence

for ^{18}O buffering of the oceans by deep (> 5 km) seawater–hydrothermal circulation of mid-ocean ridges, *J. geophys. Res.*, **86,** 2737–2755.

Hamano, Y., Bina, M.M. & Krammer, K., 1990. Palaeomagnetism of the serpentinized peridotite from ODP hole 670 A, *Proc. ODP, Scientific Results,* **106/109,** 257–262.

Harrison, C.G.A., 1987. Marine magnetic anomalies—the origin of the stripes, *Ann. Rev. Earth planet. Sci.,* **15,** 505–543.

Honnorez, J. & Kirst, P., 1975. Petrology of rodingites from the equatorial Mid-Atlantic fracture zones and their geotectonic signifiance, *Contrib. Mineral. Petrol.,* **49,** 233–257.

Horen, H., Zamora, M. & Dubuisson, G., 1996. Seismic wave velocities and anisotropy in serpentinized peridotites from Xigaze ophiolite: abundance of serpentine in slow spreading ridge, *Geophys. Res. Lett.,* **23,** 9–12.

Juteau, T., Cannat, M. & Lagabrielle, Y., 1990. Serpentinized peridotites in the upper oceanic crust away from transform zones: a comparison of the results of previous DSDP and ODP legs, *Proc. ODP, Scientific Results,* **106/109,** 303–308.

Krammer, K., 1990. Rock magnetic properties and opaque mineralogy of selected samples from Hole 670 A, *Proc. ODP, Scientific Results,* **106/109,** 269–273.

LaBrecque, J.L. & Raymond, C.A., 1985. Seafloor spreading anomalies in the Magsat field of the North Atlantic, *J. geophys. Res.,* **90,** 2565–2575.

Macdonald, K.C, 1982. Mid-ocean ridges: fine scale tectonic, volcanic and hydrothermal processes within the plate boundary zone, *Ann. Rev. Earth planet Sci.,* **10,** 155–190.

Macdonald, A.H. & Fyfe, W.S., 1985. Rate of serpentinization in seafloor environments, *Tectonophysics,* **116,** 123–135.

Moody, J.B., 1976. Serpentinization: a review, *Lithos,* **9,** 125–138.

Morris, E. & Detrick, R.S., 1991. Three-dimensional analysis of gravity anomalies in the MARK area, Mid-Atlantic Ridge 23°N, *J. geophys. Res.,* **96,** 4355–4366.

Nazarova, K.A., 1994. Serpentinized peridotites as a possible source for oceanic magnetic anomalies, *Mar. geophys. Res.,* **16,** 455–462.

Nehlig, P., 1993. Interactions between magma chambers and hydrothermal systems: oceanic and ophiolitic constraints, *J. geophys. Res.,* **98,** 19 621–19 633.

Niu, Y. & Batiza, R., 1993. Chemical variation trends at fast and slow spreading mid-ocean ridges, *J. geophys. Res.,* **98,** 7887–7902.

Pariso, J.E. & Johnson, H.P., 1993. Do lower crustal rocks records reversals of the Earth's magnetic field? Magnetic petrology of oceanic gabbros from Ocean Drilling Program Hole 735B, *J. geophys. Res.,* **98,** 16 013–16 032.

Pullaiah, G., Irving, E., Buchan, K.L. & Dunlop, D.J., 1975. Magnetization changes caused by burial and uplift, *Earth planet. Sci. Lett.,* **28,** 133–143.

Raymond, C.A. & LaBrecque, J.L., 1987. Magnetization of the oceanic crust: Thermoremanent magnetization or chemical remanent magnetization?, *J. geophys. Res.,* **92,** 8077–8088.

Roest, W.R., Arkani-Hamed, J. & Verhoef, J., 1992. The seafloor spreading rate dependence of the anomalous skewness of marine magnetic anomalies, *Geophys. J. Int.,* **109,** 653–669.

Stein, C.A. & Stein, S., 1992. A model for the global variation in oceanic depth and heat flow with lithospheric age, *Nature,* **359,** 123–129.

Talwani, M., Windisch, C.C. & Langseth, M.G., 1971. Reykjanes crest: a detailed geophysical study, *J. geophys. Res.,* **76,** 473–517.

Toft, P.B. & Arkani-Hamed, J., 1992. Magnetization of the Pacific Ocean lithosphere deduced from Magsat data, *J. geophys. Res.,* **97,** 4387–4406.

Toft, P.B., Arkani-Hamed, J. & Haggerty, S.E., 1990. The effects of serpentinization on density and magnetic susceptibility: a petrological model, *Phys. Earth planet. Inter.,* **65,** 137–157.

Verosub, K. & Moores, E.M., 1981. Tectonic rotations in extensional regimes and their paleomagnetic consequences for oceanic basalts, *J. geophys. Res.,* **86,** 6335–6349.

Wenner, D.B. & Taylor, H.P., 1971. Temperatures of serpentinization of ultramafic rocks based on O^{18}/O^{16} fractionation between coexisting serpentine and magnetite, *Contrib. Mineral. Petrol.,* **32,** 165–185.

Wicks, F.J. & O'Hanley, D.S., 1988. Serpentine minerals: Structure and petrology, in *Reviews in Mineralogy; Hydrous Phylosilicates,* Vol. 19, pp. 91–168, Book Crafters Inc., Chelsea, MI.